

Phenomenology of supersymmetric Z' decays at the Large Hadron Collider

Gennaro Corcella

*INFN - Laboratori Nazionali di Frascati
Via E. Fermi 40, I-00044, Frascati (RM), Italy*

Abstract

I study the phenomenology of heavy neutral bosons Z' , predicted in GUT-inspired $U(1)'$ models, at the Large Hadron Collider. In particular, I investigate possible signatures due to Z' decays into supersymmetric particles, such as chargino, neutralino and sneutrino pairs, leading to final states with charged leptons and missing energy. The analysis is carried out at $\sqrt{s} = 14$ TeV, for a few representative points of the parameter space of the Minimal Supersymmetric Standard Model, suitably modified to accommodate the extra Z' boson and consistent with the discovery of a Higgs-like boson with mass around 125 GeV. Results are presented for several observables and compared with those obtained for direct Z' decays into lepton pairs. For the sake of comparison, Z' production in the Sequential Standard Model and its supersymmetric decays are also investigated.

1 Introduction

Searching for heavy neutral gauge bosons Z' is one of the challenging goals of the experiments performed at the Large Hadron Collider (LHC). In fact, such bosons are predicted in extensions of the Standard Model involving an extra $U(1)'$ gauge group, inspired by Grand Unification Theories (GUTs) (see. e.g., [1, 2] for a review). Furthermore, Z' bosons are also present in the so-called Sequential Standard Model (SSM), where the Z' has the same couplings to fermions as the Standard Model (SM) Z boson. Though not being theoretically motivated, the SSM is often used as a benchmark for the experimental searches.

The LHC experiments have so far searched for high-mass neutral gauge bosons Z' and have set exclusion limits on its mass $m_{Z'}$. In detail, the ATLAS Collaboration [3] set the limits in the range $m_{Z'} > 2.22 - 2.90$ TeV for a SSM Z' and $m_{Z'} > 2.51 - 2.62$ TeV for GUT-inspired $U(1)'$ models. The same numbers for CMS [4] are instead $m_{Z'} > 2.59$ GeV for the SSM and $m_{Z'} > 2.26$ GeV in $U(1)'$ models. However, such analyses were carried out looking for high-mass dilepton pairs (e^+e^- or $\mu^+\mu^-$) and assuming that the Z' has only Standard Model decay modes. Possible decays beyond the Standard Model (BSM), e.g. in supersymmetric particles, were investigated first in [5] and lately reconsidered in [6–8] within the Minimal Supersymmetric Standard Model [9, 10]. Although SM decays are still dominant and the most promising for the searches, the opening of new decay channels decreases the branching ratios into electron and muon pairs and therefore the mass exclusion limits. Ref. [11], using a representative point of the MSSM parameter space as in [8], found that the LHC exclusion limits decrease by an amount $\Delta m_{Z'} \simeq 150\text{--}300$ GeV, once accounting for BSM decay modes at $\sqrt{s} = 8$ TeV.

From the viewpoint of supersymmetry the lack of evidence of new supersymmetric particles in the LHC runs at 7 and 8 TeV, together with the discovery of a boson with mass $m_h = 125.7 \pm 0.4$ GeV [12] and properties consistent with the Standard Model Higgs boson [13], sets some tight constraints on the mass spectra and couplings of possible supersymmetric models. While awaiting the collisions at 13 and ultimately 14 TeV, it is therefore worthwhile thinking of scenarios, not yet excluded by the current searches and compatible with the Higgs discovery, which may deserve some specific analyses at high luminosity and energy. Extending the MSSM via a $U(1)'$ group presents some features, which makes it a pretty interesting scenario, so that novel analyses, looking for signals of supersymmetric Z' decays by using current and future data, may be well justified. Unlike direct sparticle production in $q\bar{q}$ or $g\bar{g}$ annihilation, the Z' is a colourless particle and its mass sets a constraint on the invariant mass of the sparticle pair. Therefore, if one had to discover a Z' , its decay modes would be an ideal environment to look for supersymmetry, as they would yield a somewhat cleaner signal, with respect to direct production. Supersymmetric Z' decays would also be an excellent framework to study electroweak interactions in regions of the phase space which would not be accessible

through other processes, such as Drell–Yan interactions. Moreover, possible decays into pairs of the lightest neutralinos of the MSSM will lead to mono-photon or mono-jet final states, like those which are investigated when looking for Dark Matter candidates.

The reference point of the parameter space chosen in Refs. [8,11] yielded substantial decay rates into supersymmetric particles and was consistent with the present exclusion limits, but did not take into account for the recent discovery of a Higgs-like boson. In this paper I shall extend the work in [8] giving some useful benchmarks for possible Z' searches within supersymmetry. First, it will be chosen a set of points in the parameter space yielding a SM-like Higgs boson with a mass around 125 GeV. Then, thanks to the Monte Carlo implementation of the $U(1)'$ model and of the SSM, as well as of the MSSM, a phenomenological analysis will be performed and a few final-state distributions in events with supersymmetric Z' decays will be presented. On the contrary, Ref. [8] only calculated total production cross sections and branching ratios and left the investigation of differential distributions as an open issue.

In detail, in Section 2 I will shortly review the theoretical framework of the investigation here undertaken, paying special attention to the new features of the MSSM once a Z' boson is included. In Section 3 I shall discuss the practical implementation of supersymmetric Z' decays in a few computing codes and Monte Carlo event generators. Sections 4, 5 and 6 will deal with the phenomenology of the Z' in three scenarios, namely the Z'_ψ and Z'_η models, within $U(1)'$ gauge theories, and the SSM, respectively. Section 7 will contain some final remarks and comments on possible further developments of this work.

2 $U(1)'$ gauge groups and Minimal Supersymmetric Standard Model

The theoretical framework of supersymmetric Z' decays was thoroughly reviewed in [5] and, more recently, in [8]. Hereafter, for the sake of brevity, I shall just point out the essential aspects of the models, taking particular care about the new properties of the MSSM due to the extra Z' .

As discussed in [1,2], $U(1)'$ groups typically arise from the breaking of a Grand Unification gauge group E_6 of rank 6. The neutral boson Z'_ψ is associated with the group $U(1)'_\psi$, coming from the breaking into $SO(10)$ as follows:

$$E_6 \rightarrow SO(10) \times U(1)'_\psi. \quad (1)$$

The Z'_χ is instead related to the subsequent breaking of $SO(10)$ according to:

$$SO(10) \rightarrow SU(5) \times U(1)'_\chi. \quad (2)$$

The Z'_ψ and Z'_χ mix into a generic $Z'(\theta)$ depending on the mixing angle θ :

$$Z'(\theta) = Z'_\psi \cos \theta - Z'_\chi \sin \theta. \quad (3)$$

The Z'_ψ and Z'_χ models correspond to $\theta = 0$ and $\theta = -\pi/2$, respectively. Another scenario, which is often investigated from both theoretical and experimental viewpoints, is the one, characteristic of superstring theories, where E_6 breaks in the Standard Model ($SU(2)_L \times U(1)_Y$) and an extra $U(1)'$, labelled as $U(1)'_\eta$:

$$E_6 \rightarrow SM \times U(1)'_\eta. \quad (4)$$

Eq. (4) leads to a Z'_η boson, with a mixing angle $\theta = \arccos \sqrt{5/8}$ in Eq. (3). One can anticipate that the following analysis will be performed for the Z'_ψ and Z'_η models, since other models like those leading to the Z'_χ , as well as the Z'_I , Z'_S and Z'_N , corresponding to the mixing angle θ described in [8], are less interesting, as the Z' branching ratios into supersymmetric final states are rather low.

As far as the MSSM is concerned, a few relevant features are inherited by the presence of the extra Z' boson. In the Higgs sector, besides the two Higgs doublets of the MSSM, an extra singlet is necessary to break the $U(1)'$ group and give mass to the Z' . After electroweak symmetry breaking, one is then left with a novel scalar, named H' in [8], whose mass is typically larger than $m_{Z'}$. Furthermore, two extra neutralinos are present, associated with the supersymmetric partners of the Z' and of the extra Higgs bosons, for a total of six neutralinos: in [8] it was nevertheless argued that these new neutralinos are too heavy to be significant in Z' phenomenology. For the purpose of the sfermions, as debated in [5], their masses get an extra D-term correction depending on the sfermion $U(1)'$ charges and on the Higgs vacuum expectation values. This contribution to the D-term is not positive definite and therefore it may even drive to unphysical scenarios, where the sfermion squared mass gets negative (see few examples in Ref. [8]).

Besides GUT-inspired models, I will also account for the Sequential Standard Model; unlike the $U(1)'$ gauge groups, the SSM is not a real model, but nonetheless it is used by the experimental collaborations as a benchmark for the searches. In fact, if the Z' has the same couplings to the fermions as the Z , the production cross section can be straightforwardly computed as a function of the Z' mass. Following [7, 8] I will assume that even the couplings to sfermions and gauginos are the same as the Z in the MSSM. In principle, a consistent SSM should be built up along the lines of [14], wherein it was explained that any sequential Z' must be accompanied by another Z' and a longitudinal W' . However, employing this improved formulation of the SSM goes beyond the goals of this paper and therefore I shall stick to the approximations in [7, 8], with a Z'_{SM} coupled to SM and BSM particles like the Standard Model Z .

3 Framework for Z' supersymmetric decays

Hereafter, I will present a phenomenological analysis of Z' production and decay at the LHC, paying special attention to supersymmetric decay modes and comparing the results with those obtained in standard analyses, where only Standard Model channels are allowed. As discussed before, the investigation will be concentrated on the Z'_ψ , Z'_η and Z'_{SSM} models and, for each scenario, it will be chosen a point in the parameter space not yet excluded by the LHC searches and leading to an interesting Z' phenomenology within supersymmetry. In all cases, I will set the Z' mass to the value

$$m_{Z'} = 2 \text{ TeV} \quad (5)$$

and will use the following relation between $U(1)'$ and $U(1)_Y$ coupling constants g' and g_1 , typical of GUTs:

$$g' = \sqrt{\frac{5}{3}} g_1. \quad (6)$$

When dealing with the SSM, the Z' coupling constant to fermions will be the same as the Z :

$$g_{\text{SSM}} = \frac{g_2}{2 \cos \theta_W}, \quad (7)$$

where g_2 is the $SU(2)$ coupling and θ_W the Weinberg mixing angle.

In [8] the authors fixed the Z' mass and the MSSM parameters and calculated, either analytically or numerically, particle masses and Z' branching ratios into SM and MSSM final states. However, the computation was carried out at leading order (LO) in the couplings g_1 , g_2 and g' and therefore the mass of the lightest MSSM neutral Higgs boson, which roughly plays the role of the Standard Model Higgs, was around the value of the Z mass, i.e. about 90 GeV. In this paper, I shall include higher-order corrections, especially top and stop loops, in such a way to recover a light Higgs mass about 125 GeV. For this purpose, I will make use of the Mathematica package SARAH [15] which calculates the mass matrices by using renormalization group equations at one loop¹. Among the implemented models, SARAH includes the so-called UMSSM, namely the extension of the MSSM through a $U(1)'$ gauge group: the output of SARAH is used as a source code for SPheno [17] to create a precision spectrum generator for the given scenario. Model files in the Universal FeynRules Output (UFO) format [18] are then used by the MadGraph code [19] to generate the hard scattering process, with both Z' production, i.e. $q\bar{q} \rightarrow Z'$, and decay according to the chosen mode. The events are thus written in the Les Houches format and the HERWIG Monte Carlo event generator [20] can provide them with parton showers and hadronization, eventually leading to exclusive

¹The most updated SARAH version [16] even includes two-loop corrections to renormalization group equations.

final states. The analysis within the SSM is somewhat different, since SARAH and SPheno do not contain this benchmark model. A straightforward implementation can nevertheless be achieved within the package FeynRules itself [18], by simply adding to the MSSM code a Z' boson, coupled to SM and BSM particles as the Z in the Standard Model. FeynRules then constructs the UFO model files which can be read by MadGraph and HERWIG to simulate full hadron-level events.

In order to perform a consistent investigation and comparison with previous work in [5,7,8], few further changes were implemented into SARAH and FeynRules. In SARAH, I added Dirac right-handed neutrinos and sneutrinos, not present in its default version, in order to allow Z' decays into both left- and right-handed neutrino and sneutrino pairs. When modifying SARAH, the mass of the right-handed neutrino is set to zero by default. In the FeynRules implementation of the SSM, the $Z'WW$ coupling was suppressed: in fact, if one naively assumed that the Z' couples to WW pairs like the Z , on the one hand the decay $Z' \rightarrow WW$ would largely dominate, on the other the unitarity of the theory would be in trouble, because of the enhancement of WW scattering mediated by a Z' . A consistent SSM, possibly built up along the lines of [14], would not suffer from this drawback.²

In the choice of the working reference point for this investigation, I will make use of the results in [21,22], wherein the authors determined the regions of the supersymmetric phase space which are not yet excluded by the direct searches and are consistent with a Higgs of 125 GeV, taking care of the limits from flavour physics and Dark Matter searches. Stricly speaking, the results of [21,22] are obtained for the so-called phenomenological MSSM (pMSSM), which makes a few simplifying assumptions in order to reduce the number of parameters. In detail, the pMSSM assumes that the soft supersymmetry-breaking terms are real, there is no new source of CP violation, diagonal matrices for the sfermion masses and trilinear couplings, i.e. no flavour change at tree-level, same soft masses and trilinear couplings at least for the first two generations of squarks and sleptons at the electroweak scale. The leftover parameters are then the ratio of the MSSM neutral Higgs vacuum expectation values $\tan\beta = v_2/v_1$, the Higgs (higgsino) mass parameter μ , the soft masses of bino and wino M_1 and M_2 , the sfermion masses and the trilinear couplings. As in [5,8], because of the Z' , one has an extra gaugino \tilde{B}' , whose soft mass parameter is named M' .

For all the scenarios which will be studied, M_1 , M' , $\tan\beta$ and μ will be set as follows:

$$M_1 = 400 \text{ GeV} , \quad M' = 1 \text{ TeV} , \quad \tan\beta = 30 , \quad \mu = 200 \text{ GeV}. \quad (8)$$

Given M_1 , the wino mass M_2 can be obtained by using the relation $M_2 = (3/5) \cot^2 \theta_W \simeq 827 \text{ GeV}$.

²Updated releases of of SARAH and FeynRues including such changes are in progress. For the time being, the computing code to obtain the results presented in this paper can be requested from the author.

Furthermore, in the Standard Model it is well known that bottom and especially top quarks play a fundamental role in Higgs phenomenology: in fact, top loops give the highest corrections to the Higgs mass and the largest contribution to the Higgs production cross section in gluon fusion. It is therefore obvious that in the MSSM stops and sbottoms, the supersymmetric partners of top and bottom quarks, will deserve special attention and, although they have not been observed, the measured mass of the Higgs boson sets some constraints on their masses. In fact, they can be very heavy, i.e. their mass in the TeV range, but even quite light, say of the order of a few hundreds GeV, provided that the mixing is large, i.e. the mixing parameter A_t is about a few TeV (see, e.g., the discussion in [23]). The latter case is often chosen in the supersymmetry studies, namely the first two squark generations heavier than sbottoms and stops. In this paper, I shall consider both possibilities: all three squark generations heavy and generate, as well as the option of a lighter third generation. The authors of [21] define the mixing parameter:

$$x_t = A_t - \mu \cot \beta, \quad (9)$$

which runs in the range $0 < x_t < \sqrt{6} M_S$, M_S being the geometrical average of the stop masses, i.e. $M_S = \sqrt{m_{\tilde{t}_1} m_{\tilde{t}_2}}$, where $m_{\tilde{t}_1}$ and $m_{\tilde{t}_2}$ are obtained after adding to the soft mass m_t^0 the D-term (see [5]) and diagonalizing the stop mixing matrix.

In Eq. (9), A_t is a dimensionful quantity related to the dimensionless trilinear coupling $A_{t,0}$ in [8] via $A_t = A_{t,0} m_t$, where m_t is the top quark mass, which will be fixed to $m_t = 173$ GeV. For $x_t = 4$ TeV, one obtains that, using the numbers in (8), $A_t \simeq 4$ TeV and $A_{t,0} \simeq 23.2$. Later on, all the trilinear couplings, as well as A_λ , contained in the scalar-potential term involving the neutral components of the three Higgs bosons ($V_\lambda = \lambda A_\lambda \phi_1^0 \phi_2^0 \phi_3^0$) will be equal to A_t :³

$$A_q = A_\ell = A_\lambda \simeq 4 \text{ TeV}. \quad (10)$$

In the following sections, I shall present the results yielded at the LHC by the models $U(1)'_\psi$, $U(1)'_\eta$ and, for the sake of comparison, by the SSM. In [8], a few decay chains were taken into account: they all started with a primary supersymmetric decay, i.e. into pairs of charged sleptons, sneutrinos, charginos or neutralinos, and eventually yielded final states with two or four charged leptons and missing transverse energy (MET), associated with neutrinos or light neutralinos. For each model, I will consider a specific point in the parameter space, with the goal of maximizing the branching ratio in at least one of the supersymmetric modes, eventually leading to leptons and missing energy. Then, I shall present some leptonic final-state distribution, in the scenario which maximizes the BSM Z' decay rate. Whenever the comparison is consistent, the results will be confronted with those from the standard search strategy, where the Z' directly decays into a SM charged-lepton pair and has no BSM decay width.

³Note that SARAH requires $A_\lambda/\sqrt{2} \simeq 2.8$ TeV as an input, rather than A_λ in Eq. (10).

4 Phenomenology - $U(1)'_\psi$ model

The model $U(1)'_\psi$ leads to a heavy boson Z'_ψ , corresponding to a mixing angle $\theta = 0$ in Eq. (3). In [8], it was found that, in a reference point of the parameter space and for a Z'_ψ mass between 1 and 5 TeV, about 35% of the Z'_ψ width is due to the supersymmetric modes. However, as discussed above, that scenario was not consistent with a Higgs mass of 125 GeV and the supersymmetric mass spectrum was computed only at tree level.

Hereafter, the representative points of the parameter space will be chosen in order to satisfy the Higgs mass constraint and the supersymmetry exclusion limits. The quantities M_1 , M' , μ and $\tan\beta$ are fixed as in Eq. (8); as for sfermions, I assume that sleptons, as well as the first two generations of squarks, are degenerate at the Z'_ψ mass scale and have mass ⁴:

$$m_\ell^0 = m_{\tilde{\nu}_\ell}^0 = 1.2 \text{ TeV} , \quad m_{\tilde{q}}^0 = 5.5 \text{ TeV} , \quad (11)$$

where $\ell = e, \mu, \tau$, $\nu = \nu_e, \nu_\mu, \nu_\tau$ and $q = u, d, c, s$. The soft masses of stops and sbottoms are instead fixed as follows:

$$m_{\tilde{t}}^0 = m_{\tilde{b}}^0 = 2.2 \text{ TeV} . \quad (12)$$

The sfermion masses at the Z'_ψ mass scale are obtained after summing to the numbers in (11) and (12) the D-terms due to $U(1)'$ and electroweak symmetry breaking. The equations for the D-term correction to the masses of up- and down-type squarks and sleptons are given in [5] and will not be reported here for the sake of brevity; at leading order the masses yielded by the SARAH code agree with those computed by using the expressions in [5]. For $m_{Z'} = 2 \text{ TeV}$, the sfermion masses are quoted in Tables 1 and 2, for squarks and sleptons, respectively. The notation $\tilde{q}_{1,2}$, $\tilde{\ell}_{1,2}$ and $\tilde{\nu}_{1,2}$ refers to the mass eigenstates, which differ from the gauge ones $\tilde{q}_{L,R}$, $\tilde{\ell}_{L,R}$ and $\tilde{\nu}_{L,R}$ because of the mixing; the mixing terms are proportional to the fermion squared masses, and therefore they are mostly relevant in the case of the stops. From such tables, one can learn that the impact of the D-term is about 100 GeV on squarks and even larger than 200 GeV on sleptons; also, in the chosen reference point, the D-term can be either positive or negative.

In the Higgs sector, there will be three neutral scalars (h , H and H'), where h and H are the usual MSSM ones and H' is the extra $U(1)'$ -inherited one, a pseudoscalar A and a pair of charged H^\pm ; The Higgs masses, computed by SARAH at one loop, are reported in Table 3. The lightest scalar h has roughly the mass of the SM-like Higgs boson, H is approximately as heavy as the Z'_ψ , whereas H' , A and the charged H^\pm are above 4 TeV, and therefore too heavy to be significant for Z'_ψ phenomenology. The

⁴Alternatively, one can fix the sfermion masses at a very high scale, such as the Planck mass, and then evolve them down to the Z' scale by means of renormalization group equations

λ parameter, contained in the trilinear potential V_λ , is related to μ and the vacuum expectation value v_3 of the extra Higgs boson Φ_3 via $\lambda = \sqrt{2}\mu/v_3 \simeq 5.4 \times 10^{-2}$. Table 4 contains the masses of the two charginos ($\tilde{\chi}_{1,2}^\pm$) and of the six neutralinos ($\tilde{\chi}_1^0, \dots, \tilde{\chi}_6^0$): in principle, with the exception of $\tilde{\chi}_6^0$, whose mass is even above 6 TeV, several Z'_ψ decay modes into pairs of charginos and neutralinos are kinematically permitted.

Given the numbers in Tables 1–4, one can calculate, by means of the SPheno program, the branching ratios of the Z'_ψ into Standard Model and supersymmetric final states. At leading order in g' , i.e. $\mathcal{O}(g'^2)$, the main Z'_ψ branching ratios are quoted in Table 5, for $m_{Z'} = 2$ TeV and omitting decay rates which are below 0.1%. The Standard Model decays are still the dominant ones, but one has an overall 28.3% branching ratio into supersymmetric final states, which deserves further investigation. In particular, the decay into chargino pairs $\tilde{\chi}_1^+ \tilde{\chi}_1^-$ accounts for about 10%, whereas the ratios into neutralino pairs vary from 0.2% ($\tilde{\chi}_1^0 \tilde{\chi}_3^0$) to 8% ($\tilde{\chi}_4^0 \tilde{\chi}_4^0$). Decays into pairs of the lightest neutralinos, i.e. $\tilde{\chi}_1^0 \tilde{\chi}_1^0$, relevant for the searches for Dark Matter candidates, have non-negligible branching ratio, accounting for about 5%.

Since the highest BSM rate is the one into chargino pairs, it is worthwhile carrying out the phenomenological analysis for final states originated from a $Z'_\psi \rightarrow \tilde{\chi}_1^+ \tilde{\chi}_1^-$ process. As discussed in [8], primary decays into chargino pairs can lead to a chain yielding charged leptons and missing energy in the final states. To gauge the rates of the different final states, one must compute the branching ratios of the 2- and 3-body decays of the charginos $\tilde{\chi}_1^\pm$. These numbers, calculated by means of SPheno, are quoted in Table 6. As hadronic final states are likely affected by large QCD backgrounds, I shall focus on the modes with neutralinos and leptons, which will eventually lead to the following decay chain:

$$pp \rightarrow Z'_\psi \rightarrow \tilde{\chi}_1^+ \tilde{\chi}_1^- \rightarrow (\tilde{\chi}_1^0 \ell^+ \nu_\ell)(\tilde{\chi}_1^0 \ell^- \bar{\nu}_\ell), \quad (13)$$

with $\ell = \mu, e$. The neutrinos and neutralinos in (13) will give rise to some missing

Table 1: Masses of squarks in the MSSM, for the chosen reference point and accounting for the $U(1)'_\psi$ modifications. The masses of $\tilde{q}_{1,2}$ differ from those of the gauge eigenstates $\tilde{q}_{L,R}$ because of the mixing contribution, relevant especially in the stop case. All numbers are expressed in GeV.

$m_{\tilde{d}_1}$	$m_{\tilde{u}_1}$	$m_{\tilde{s}_1}$	$m_{\tilde{c}_1}$	$m_{\tilde{b}_1}$	$m_{\tilde{t}_1}$
5609.8	5609.4	5609.9	5609.5	2321.7	2397.2
$m_{\tilde{d}_2}$	$m_{\tilde{u}_2}$	$m_{\tilde{s}_2}$	$m_{\tilde{c}_2}$	$m_{\tilde{b}_2}$	$m_{\tilde{t}_2}$
5504.9	5508.7	5504.9	5508.7	2119.6	2036.3

Table 2: As in Table 1, but for charged sleptons ($\ell = e, \mu$) and sneutrinos.

$m_{\tilde{\ell}_1}$	$m_{\tilde{\ell}_2}$	$m_{\tilde{\tau}_1}$	$m_{\tilde{\tau}_2}$	$m_{\tilde{\nu}_{\ell,1}}$	$m_{\tilde{\nu}_{\ell,2}}$	$m_{\tilde{\nu}_{\tau,1}}$	$m_{\tilde{\nu}_{\tau,2}}$
1392.4	953.0	1398.9	971.1	1389.8	961.5	1395.9	961.5

Table 3: Masses of neutral and charged Higgs bosons in GeV in the chosen point of the MSSM extended by means of the $U(1)'_{\psi}$ gauge model.

m_h	m_H	$m_{H'}$	m_A	$m_{H^{\pm}}$
125.0	1989.7	4225.0	4225.0	4335.6

Table 4: Masses of charginos and neutralinos in the reference point for the Z'_{ψ} model, in GeV.

$m_{\tilde{\chi}_1^+}$	$m_{\tilde{\chi}_2^+}$	$m_{\tilde{\chi}_1^0}$	$m_{\tilde{\chi}_2^0}$	$m_{\tilde{\chi}_3^0}$	$m_{\tilde{\chi}_4^0}$	$m_{\tilde{\chi}_5^0}$	$m_{\tilde{\chi}_6^0}$
204.8	889.1	197.2	210.7	408.8	647.9	889.0	6193.5

Table 5: Z'_ψ decay rates for $m'_Z = 2$ TeV.

Final State	Z'_ψ Branching ratio (%)
$\tilde{\chi}_1^+ \chi_1^-$	10.2
$\tilde{\chi}_1^0 \tilde{\chi}_1^0$	4.9
$\tilde{\chi}_1^0 \tilde{\chi}_3^0$	0.2
$\tilde{\chi}_2^0 \tilde{\chi}_2^0$	5.1
$\tilde{\chi}_4^0 \tilde{\chi}_4^0$	8.0
hZ	1.4
$W^+ W^-$	2.9
$\sum_i d_i \bar{d}_i$	25.1
$\sum_i u_i \bar{u}_i$	25.0
$\sum_i \nu_i \bar{\nu}_i$	8.3
$\sum_i \ell_i^+ \ell_i^-$	8.3

Table 6: Chargino $\tilde{\chi}_1^+$ decay rates in the reference point for the Z'_ψ model.

Final State	χ_1^+ branching ratio (%)
$\tilde{\chi}_1^0 u \bar{d}$	34.3
$\tilde{\chi}_1^0 u \bar{c}$	1.8
$\tilde{\chi}_1^0 c \bar{d}$	1.6
$\tilde{\chi}_1^0 c \bar{s}$	29.3
$\tilde{\chi}_1^0 e^+ \nu_e$	12.0
$\tilde{\chi}_1^0 \mu^+ \nu_\mu$	12.0
$\tilde{\chi}_1^0 \tau^+ \nu_\tau$	8.9

energy; the diagram of such a process is presented in Fig. 1. The $U(1)'_\psi/\text{MSSM}$ model, in the UFO format, can be used by MadGraph to generate parton-level events and then by HERWIG to simulate showers and hadronization. The cross section for the process $pp \rightarrow Z'_\psi$, computed by MadGraph at LO, by using the CTEQL1 set [24] for the initial-state parton distributions and $m_{Z'} = 2$ TeV, is $\sigma(pp \rightarrow Z') \simeq 0.13$ pb. The cross section for the decay chain (13) is then given by: $\sigma(pp \rightarrow Z'_\psi \rightarrow \ell^+ \ell^- + \text{MET}) \simeq 7.9 \times 10^{-4}$ pb at 14 TeV. This means that such events can be, e.g., about 80 for a luminosity $\mathcal{L} \simeq 100 \text{ fb}^{-1}$, almost 240 at 300 fb^{-1} and so on. Though being less likely than SM channels, supersymmetric decays lead to pretty different final states which, if the Z' mass is known, have a fixed invariant mass.

In the following, I will present some relevant leptonic distributions and, whenever the comparison makes sense, the results will be shown for both direct decays $Z' \rightarrow \ell^+ \ell^-$ and the cascade (13). Fig. 2 presents the transverse momentum spectrum of leptons produced in both processes: as the production of ℓ^+ and ℓ^- is symmetric, the histograms contain the p_T of both leptons. For direct production, the p_T distribution starts to be non-negligible for $p_T > 200$ GeV, i.e. about $m_{Z'}/10$, then increases and reaches a peak about $p_T \simeq 1 \text{ TeV} = m_{Z'}/2$; above 1 TeV the spectrum rapidly decreases. On the contrary, in the case of the decay chain (13), the lepton transverse momentum has a completely different behaviour: it increases in the low range and reaches its peak at $p_T \simeq 15$ GeV, then it smoothly decreases, in such a way that there are nearly no

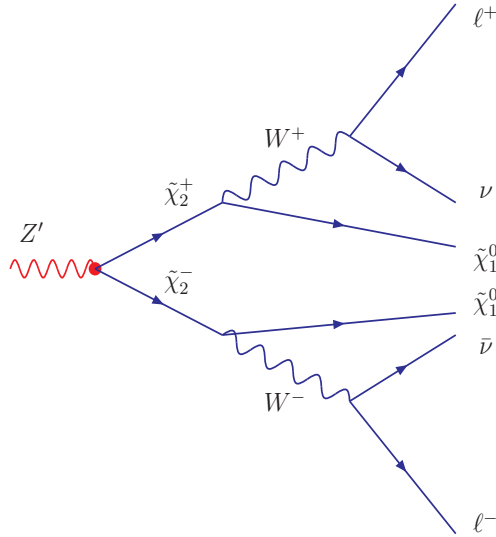


Figure 1: Final state with two charged leptons and missing energy, due to neutrinos and neutralinos, through a primary decay of the Z' into a chargino pair.

events with leptons with $p_T > 60$ GeV. The observed spectra can be easily understood, since in one case the two leptons get the full initial-state transverse momentum, whereas, in the case of the cascade, a consistent (missing) p_T is lent to neutrinos and neutralinos, which significantly decreases the p_T of ℓ^+ and ℓ^- .

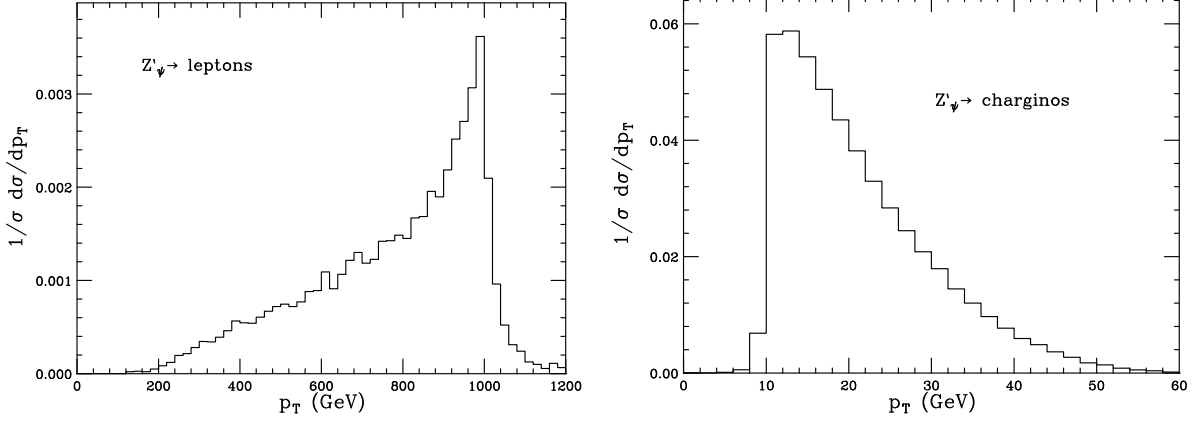


Figure 2: Lepton transverse momentum for the Z'_ψ model at $\sqrt{s} = 14$ TeV and $m_{Z'} = 2$ TeV, for a direct $Z'_\psi \rightarrow \ell^+ \ell^-$ decay (left) and a chain initiated by a $Z'_\psi \rightarrow \tilde{\chi}_1^+ \tilde{\chi}_1^-$ (right).

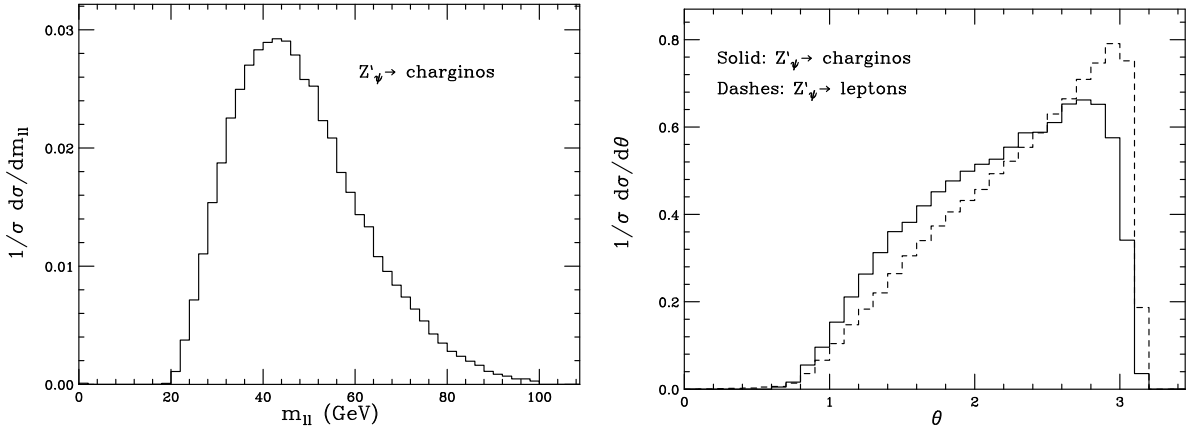


Figure 3: Left: $\ell^+ \ell^-$ invariant mass distribution for leptons coming from a primary $Z'_\psi \rightarrow \tilde{\chi}_1^+ \tilde{\chi}_1^-$ decay. Right: angle between the two leptons ℓ^\pm and in the laboratory frame for direct $Z'_\psi \rightarrow \ell^+ \ell^-$ production (dashes) and after the decay chain in Eq. (13) (solid histogram).

In Fig. 3 one can instead find the invariant mass $m_{\ell\ell}$ (left) and the angle θ between the two charged leptons in the laboratory frame (right). The invariant mass is plotted

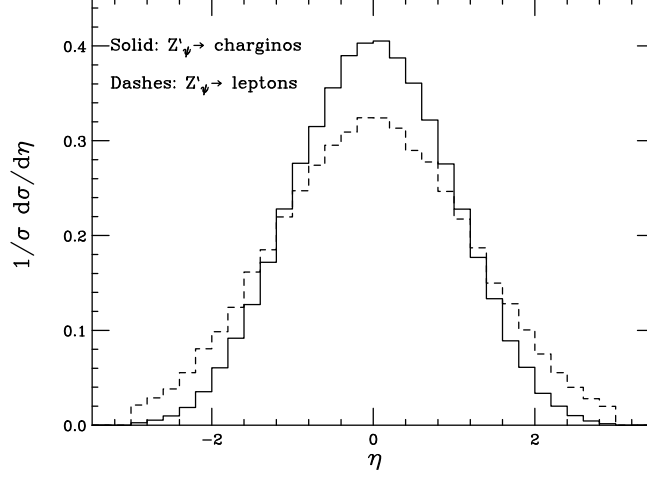


Figure 4: Lepton rapidity distributions for standard Z'_ψ decays into lepton pairs (dashes) and in the supersymmetric cascade, initiated by charginos (solid histogram).

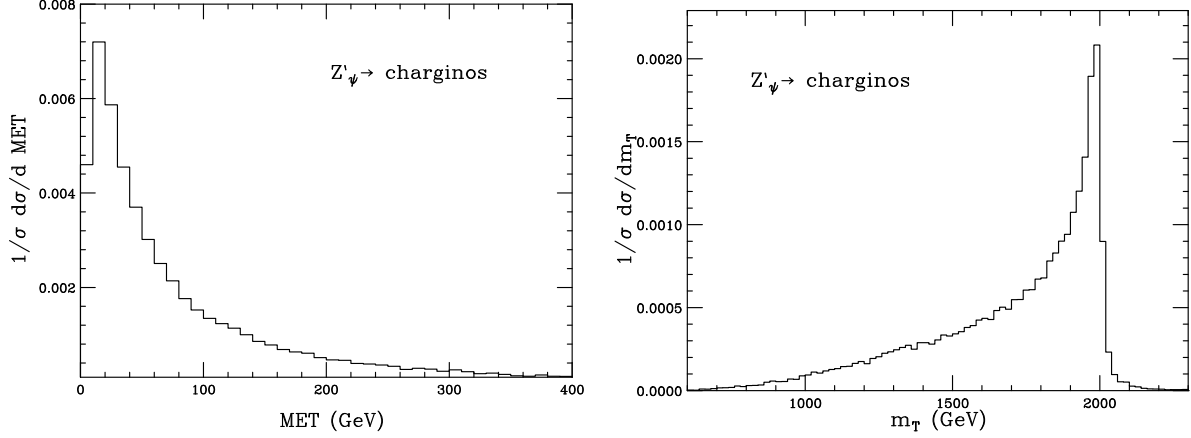


Figure 5: Left: missing transverse energy due to the neutrinos and neutralinos in the cascade initiated by a primary $Z'_\psi \rightarrow \tilde{\chi}_1^+ \tilde{\chi}_1^-$ decay. Right: transverse mass for the final-state particles (leptons, neutrinos and neutralinos) in the reaction (13).

only for the cascade (13), since, for direct $Z'_\psi \rightarrow \ell^+\ell^-$, it would just be a narrow resonance with the same mass and width as the Z'_ψ . When the leptons come from the process in Eq. (13), their invariant mass does not have to reproduce the Z' ; it varies essentially in the range $20 \text{ GeV} < m_{\ell\ell} < 100 \text{ GeV}$ and has its maximum value about $m_{\ell\ell} \simeq 45 \text{ GeV}$. The θ spectrum, in the case of direct production, exhibits a maximum about $\theta \simeq 3$, a value close to back-to-back production, i.e. $\theta = \pi$. When the leptons are accompanied by missing energy, the θ distribution is broader, lies above the direct-production spectrum at small and middle angles, below at high θ , and is peaked at a lower $\theta \simeq 2.75$. Fig. 4 presents the ℓ^\pm rapidity distributions: the η spectrum for leptons originated from a supersymmetric cascade presents more events at $\eta = 0$, corresponding to production perpendicular to the beam axis, whereas one has a higher probability of leptons at small angle with respect to the beam, i.e. large values of $|\eta|$, when they come from a primary $Z'_\psi \rightarrow \ell^+\ell^-$ process. Fig. 5 presents the differential distributions of two observables which are typically studied in supersymmetry searches: the sum of the transverse momenta of ‘invisible’ particles like neutrinos and neutralinos, also called MET (missing transverse energy), and the transverse mass m_T of all final-state particles (neutrinos, neutralinos and charged leptons) in (13). They are defined as follows:

$$\begin{aligned} \text{MET} &= \sqrt{\left(\sum_i p_{x,i}\right)^2 + \left(\sum_i p_{y,i}\right)^2} \quad , \quad i = \nu, \bar{\nu}, \tilde{\chi}_1^0 ; \\ m_T &= \sqrt{\left(\sum_j E_{T,j}\right)^2 - \left(\sum_j \vec{p}_{T,j}\right)^2} \quad , \quad E_{T,j} = \sqrt{m_j^2 + p_{T,j}^2} \quad , \quad j = \ell^+, \ell^-, \nu, \bar{\nu}, \tilde{\chi}_1^0. \end{aligned} \quad (14)$$

The MET spectrum is significant essentially in the low range: it is sharply peaked at $\text{MET} \simeq 15 \text{ GeV}$ and smoothly decreases so that for $\text{MET} > 300 \text{ GeV}$ there are nearly no events. The transverse mass distribution exhibits instead an opposite behaviour: it is relevant in the range $m_{Z'}/2 < m_T < m_{Z'}$ and presents a sharp peak at $m_T \simeq 1.8 \text{ TeV}$, just below the Z'_ψ mass threshold.

Since the Z'_ψ branching ratio into neutralino pairs $\tilde{\chi}_1^0 \tilde{\chi}_1^0$ is almost 5%, even the process

$$pp \rightarrow Z'_\psi \rightarrow \tilde{\chi}_1^0 \tilde{\chi}_1^0 \quad (15)$$

has a non-negligible cross section, i.e. $\sigma(pp \rightarrow Z'_\psi \rightarrow \text{MET}) \simeq 6.4 \times 10^{-3} \text{ pb}$, which yields about 640 events at $\mathcal{L} = 100 \text{ fb}^{-1}$ and up to almost 2×10^3 at 300 fb^{-1} . In fact, unlike charginos, the lightest neutralinos are stable particles in the MSSM, and therefore the cross section of the process (15) does not get any further branching fraction which possibly decreases the event rate. Therefore, the $U(1)'_\psi$ extension of the MSSM could be an interesting scenario to search for Dark Matter candidates in the 14 TeV run of the LHC. The typical signature is given by mono-photon or mono-jet final states, with the photon and jet being associated to the initial-state radiation from the incoming quarks. The actual implementation of photon isolation criteria or jet-clustering algorithms goes

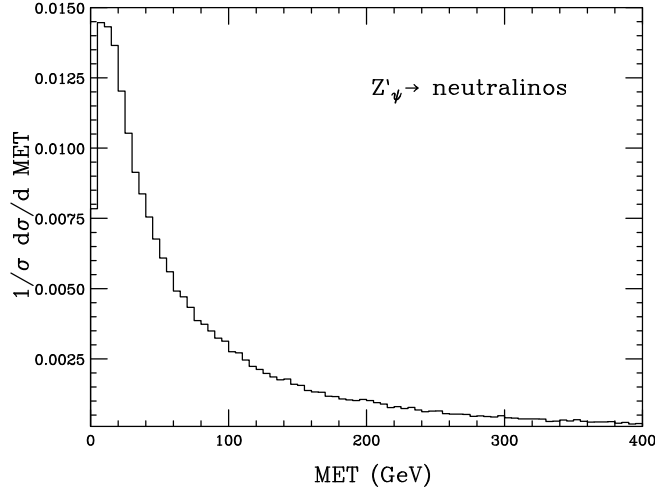


Figure 6: Missing transverse energy in Z'_ψ decays into pairs of the lightest neutralinos of the MSSM.

beyond the scopes of this paper and will not be debated here. Nevertheless, Fig. 6 displays the missing transverse energy (MET) due to the neutralinos in the final state in (15). The neutralino MET distribution is peaked at $\text{MET} \simeq 10$ GeV and smoothly decreases, up to the point of being quite negligible for $\text{MET} > 300$ GeV.

5 Phenomenology - $U(1)'_\eta$ model

The model $U(1)'_\eta$ corresponds to a mixing angle $\theta = \arccos \sqrt{5/8}$ and, even in the reference point considered in [8], gives rise to an interesting Z'_η phenomenology within supersymmetry, accounting for about 1/4 of the total width. In the following, though keeping the constraints due to the Higgs mass and direct supersymmetry searches, I shall choose a slightly different representative point of the parameter space, with respect to the previous $U(1)'_\psi$ model, in order to possibly enhance supersymmetric Z'_η decays. In particular, the Z'_η will still have mass $m_{Z'} = 2$ TeV, M_1 , M_2 , M' , $\tan \beta$, μ , A_q , A_ℓ and A_λ will be set to the values in Eqs. (8) and (10), like in the Z'_ψ scenario, whereas all three generations of squarks and sleptons will be degenerate at the Z'_η scale, with masses equal to the following values:

$$m_{\tilde{\ell}}^0 = m_{\tilde{\nu}_\ell}^0 = 1.5 \text{ TeV} , \quad m_{\tilde{q}}^0 = 3 \text{ TeV} , \quad (16)$$

where $q = u, d, c, s, t, b$ and $\ell = e, \mu, \tau$. After adding the D-term, the masses of squarks and sleptons are those quoted in Tables 7 and 8, exhibiting a substantial impact of the D-term. The squark masses increase or decrease by few hundreds GeV, whereas $\tilde{\ell}_2$ and $\tilde{\nu}_1$

get slightly heavier, $m_{\tilde{\ell}_2}$ a bit lower and $\tilde{\nu}_2$ considerably lighter, by about 850 GeV. This is therefore an example of negative D-term; in the scenarios investigated in [8], negative and large D-terms have even led to the exclusion of a few Z' models, as some sfermion squared masses had become negative, and therefore unphysical. Table 9 contains the masses of the Higgs bosons, which are rather similar to those obtained for the Z'_ψ case: $m_h \simeq 125$ GeV, $m_H \simeq m_{Z'}$ and the masses of H' , A and H^\pm are above 4 TeV. With those numbers for the Higgs boson, the λ parameter in the trilinear potential V_λ is now equal to $\lambda = \sqrt{2}\mu/v_3 \simeq 4.3 \times 10^{-2}$. Chargino and neutralino masses are reported in Table 10: the two charginos ($\tilde{\chi}_1^\pm$ and $\tilde{\chi}_2^\pm$) and the first four neutralinos ($\tilde{\chi}_1^0 \dots \tilde{\chi}_4^0$) are roughly as heavy as those in the Z'_ψ model previously considered; $\tilde{\chi}_5^0$ and $\tilde{\chi}_6^0$ have masses above 1.5 and 2.5 TeV, respectively, and, being so heavy, are quite negligible for Z'_η phenomenology.

Table 7: Masses in GeV of the squarks in the Z'_η model in the representative point of the parameter space, for a soft mass $m_{\tilde{q}}^0 = 3$ TeV and $m_{Z'} = 2$ TeV.

$m_{\tilde{d}_1}$	$m_{\tilde{u}_1}$	$m_{\tilde{s}_1}$	$m_{\tilde{c}_1}$	$m_{\tilde{b}_1}$	$m_{\tilde{t}_1}$
3130.8	3129.8	3130.8	3129.8	3130.8	3175.5
$m_{\tilde{d}_2}$	$m_{\tilde{u}_2}$	$m_{\tilde{s}_2}$	$m_{\tilde{c}_2}$	$m_{\tilde{b}_2}$	$m_{\tilde{t}_2}$
3065.9	2863.6	3065.9	2863.6	3065.9	2823.5

Table 8: Masses of sleptons in the Z'_η scenario, with a soft term $m_\ell^0 = m_{\tilde{\nu}} = 1.3$ TeV. All numbers are in GeV and $\ell = e, \mu$.

$m_{\tilde{\ell}_1}$	$m_{\tilde{\ell}_2}$	$m_{\tilde{\tau}_1}$	$m_{\tilde{\tau}_2}$	$m_{\tilde{\nu}_{\ell,1}}$	$m_{\tilde{\nu}_{\ell,2}}$	$m_{\tilde{\nu}_{\tau,1}}$	$m_{\tilde{\nu}_{\tau,2}}$
1194.6	1364.5	1208.8	1307.7	1361.8	456.0	1368.0	456.05

Table 11 presents the branching ratios of the Z'_η into the most significant decay channels: the Standard Model modes are still the most relevant ones, with the supersymmetric channels accounting for about 21% of the total width. Among the supersymmetric channels the one into sneutrino pairs $\tilde{\nu}_2 \tilde{\nu}_2^*$ exhibits the highest rate, slightly below 10% after adding up all three flavours, whereas the decay into $\tilde{\chi}_1^+ \tilde{\chi}_1^-$ accounts for about 6% and those into neutralino pairs for another 5%. As done for the purpose of the previous model, the phenomenological analysis will be undertaken for the supersymmetric mode with the highest branching ratio, i.e. $Z'_\eta \rightarrow \tilde{\nu}_2 \tilde{\nu}_2^*$. In the notation used in this paper, $\tilde{\nu}_2$ is

Table 9: Higgs bosons in the Z'_η model, with masses expressed in GeV.

m_h	m_H	$m_{H'}$	m_A	m_{H^+}
124.9	2004.2	4229.4	4229.4	4230.0

Table 10: Masses in GeV of charginos and neutralinos in the Z'_η model.

$m_{\tilde{\chi}_1^+}$	$m_{\tilde{\chi}_2^+}$	$m_{\tilde{\chi}_1^0}$	$m_{\tilde{\chi}_2^0}$	$m_{\tilde{\chi}_3^0}$	$m_{\tilde{\chi}_4^0}$	$m_{\tilde{\chi}_5^0}$	$m_{\tilde{\chi}_6^0}$
206.5	882.4	199.3	212.5	408.2	882.3	1562.8	2569.2

Table 11: Z'_η decay rates in the MSSM reference point for a mass $m_{Z'} = 2$ TeV.

Final State	Z' Branching ratio (%)
$\tilde{\chi}_1^+ \chi_1^-$	5.6
$\tilde{\chi}_1^0 \tilde{\chi}_1^0$	1.9
$\tilde{\chi}_2^0 \tilde{\chi}_2^0$	2.1
$\tilde{\chi}_1^0 \tilde{\chi}_2^0$	1.5
$\sum_\ell \tilde{\nu}_{\ell,2} \tilde{\nu}_{\ell,2}^*$	9.4
hZ	1.5
$W^+ W^-$	3.0
$\sum_i d_i \bar{d}_i$	16.1
$\sum_i u_i \bar{u}_i$	25.5
$\sum_i \nu_i \bar{\nu}_i$	27.8
$\sum_i \ell_i^+ \ell_i^-$	5.3

Table 12: Sneutrino $\tilde{\nu}_2$ branching ratios, in the representative point of the Z'_η model, where $m_{\tilde{\nu}_2} \simeq 456$ GeV.

Final State	$\tilde{\nu}_2$ Branching ratio (%)
$\tilde{\chi}_1^0 \nu_2$	4.0
$\tilde{\chi}_2^0 \nu_2$	37.3
$\tilde{\chi}_3^0 \nu_2$	58.7

the supersymmetric partner of the ν_2 , which, after the mixing, is mostly a right-handed neutrino. The sneutrinos decay into neutrinos and neutralinos, with branching ratios given in Table 12: according to whether the neutralino is a $\tilde{\chi}_3^0$, $\tilde{\chi}_2^0$ or a $\tilde{\chi}_1^0$, the decay rate varies from 4% to almost 60%. Following [8], an interesting cascade, leading to a final state with leptons and missing energy, is the one driven by the decay $\tilde{\nu}_2 \rightarrow \tilde{\chi}_2^0 \nu_2$, followed by a decay of $\tilde{\chi}_2^0$ into the lightest $\tilde{\chi}_1^0$ and a pair of charged leptons, through an intermediate charged slepton $\tilde{\ell}^\pm$, as in Fig. 5. In other words, I shall investigate the following decay chain:

$$pp \rightarrow Z'_\eta \rightarrow \tilde{\nu}_2 \tilde{\nu}_2^* \rightarrow (\tilde{\chi}_2^0 \nu_2)(\tilde{\chi}_2^0 \bar{\nu}_2) \rightarrow (\ell^+ \ell^- \tilde{\chi}_1^0 \nu_2)(\ell^+ \ell^- \tilde{\chi}_1^0 \bar{\nu}_2). \quad (17)$$

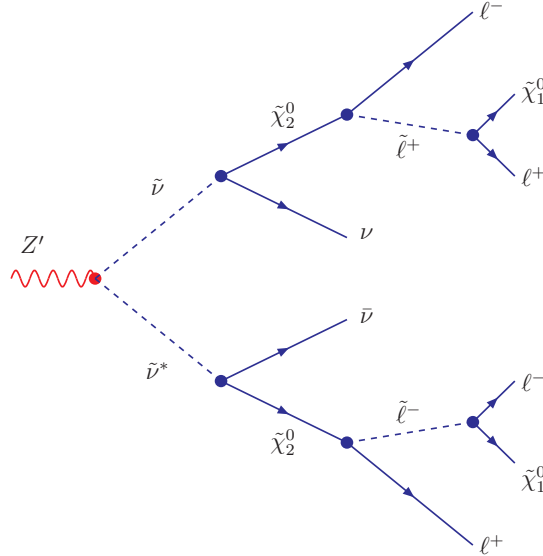


Figure 7: Final state with four charged leptons and missing energy, initiated by a Z' decay into a sneutrino pair.

Table 13: Branching ratios of the neutralino $\tilde{\chi}_2^0$ in the representative point of the Z'_η model.

Final State	$\tilde{\nu}_2$ Branching ratio (%)
$\sum_i \tilde{\chi}_1^0 q_i \bar{q}_i$	63.3
$\sum_i \tilde{\chi}_1^0 \ell_i^+ \ell_i^-$	13.4
$\sum_i \tilde{\chi}_1^0 \nu_i \bar{\nu}_i$	20.6

The final state of the cascade (17) is then made of four charged leptons and missing energy, because of two light neutralinos and two neutrinos. The main branching fractions of $\tilde{\chi}_2^0$ are quoted in Table 13: the rate in final states with the lightest neutralino $\tilde{\chi}_1^0$ and a charged-lepton pair, interesting to recover the event in Fig. 17, is about 13%, with a fraction 2/3, i.e. nearly 9%, leading to final-state electrons or muons. The cross section for Z'_η production in the above scenario at 14 TeV, computed by MadGraph, is $\sigma(pp \rightarrow Z'_\eta) \simeq 0.18$ pb. Given the numbers in Tables 12 and 13, and accounting only for e^\pm and μ^\pm , the cross section of the cascade (17) is thus $\sigma(pp \rightarrow Z'_\eta \rightarrow 4\ell + \text{MET}) \simeq 1.90 \times 10^{-4}$ pb, which yields about 20 events at $\mathcal{L} = 100 \text{ fb}^{-1}$ and 60 at 300 fb^{-1} .

In Fig. 8 the lepton transverse momenta in the decay chain (17) and in direct decays $Z'_\eta \rightarrow \ell^+ \ell^-$ are plotted: unlike the Z'_ψ case, where we had final states with two charged leptons, with roughly the same kinematic properties, the decay chain (17) presents four leptons, with different kinematics. Therefore, in Fig. 8, on the left-hand side we have the spectra in p_T of the hardest (solid) and softest (dashes) lepton in the cascade (17), on the right-hand side the p_T of ℓ^\pm in $Z'_\eta \rightarrow \ell^+ \ell^-$. In the cascade, the hardest lepton has a broad spectrum, relevant in the $10 \text{ GeV} < p_T < 50 \text{ GeV}$ range and maximum around $p_T \simeq 20\text{-}25 \text{ GeV}$; the p_T of the softest ℓ^\pm is instead a narrow distribution, substantial only for $8 \text{ GeV} < p_T < 20 \text{ GeV}$ and sharply peaked at $p_T \simeq 11 \text{ GeV}$. The spectrum in direct production $Z'_\eta \rightarrow \ell^+ \ell^-$ is roughly the same as in the Z'_ψ case: in fact, using normalized distributions like $(1/\sigma) d\sigma/dp_T$ minimizes the impact of the value of the coupling. In Fig. 9, I have instead included two invariant-mass spectra: $m_{4\ell}$, the invariant mass of the four charged leptons in (17), and $m_{\ell\ell}$, invariant mass of the $\ell^+ \ell^-$ pairs in secondary $\chi_2^0 \rightarrow \chi_1^0 \ell^+ \ell^-$ processes, assuming that one is ideally able to identify and reconstruct the leptons coming from each $\tilde{\chi}_2^0$ decay.

The $m_{\ell\ell}$ spectrum is significant only in the range $4 \text{ GeV} < m_{\ell\ell} < 13 \text{ GeV}$ and peaked around $m_{\ell\ell} \simeq 9 \text{ GeV}$; $m_{4\ell}$ is relevant between 40 and 150 GeV and is maximum at $m_{4\ell} \simeq 70 \text{ GeV}$. Finally, Fig. 10 presents the spectrum of the missing transverse energy and transverse mass of the final states in the process in Fig. 5, defined as in Eq. (14). The MET distribution is similar to the Z'_ψ one, peaked at 20 GeV and decreasing quite rapidly

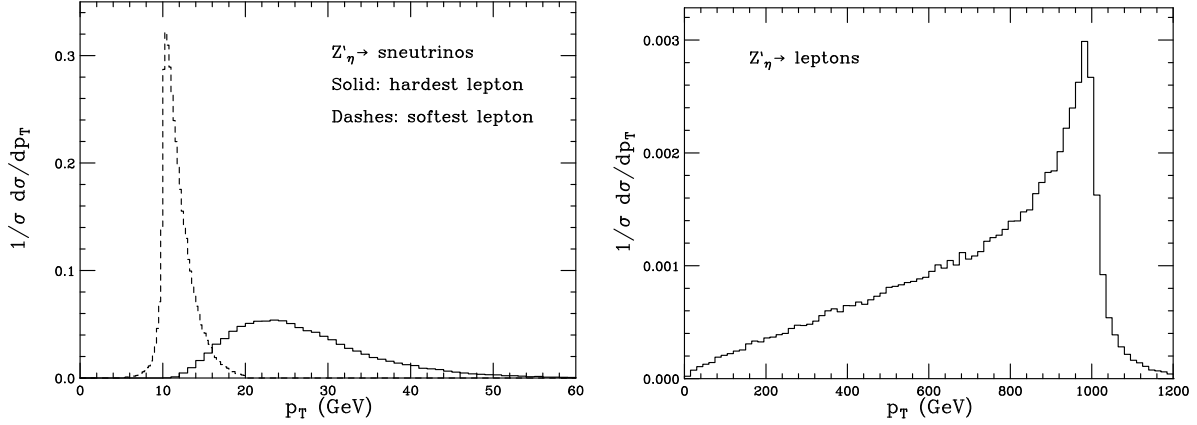


Figure 8: Left: Transverse momentum of the hardest (solid) and softest (dashes) lepton in the cascade (17). Right: Lepton transverse momentum in $Z'_\eta \rightarrow \ell^+ \ell^-$ processes.

for larger MET values; the transverse mass is relevant in the range $m_{Z'}/2 < m_T < m_{Z'}$ and is overall a broader and smoother distribution with respect to the previous model, with a peak still around $m_T \simeq 1.8$ TeV.

6 Phenomenology - Sequential Standard Model

The Sequential Standard Model (SSM) is the simplest extension of the Standard Model, since it just contains Z' and possibly W' bosons, with the same couplings to fermions as the Standard Model Z and W . Although it does not have any strong theoretical motivation, as happens for GUT-inspired gauge symmetries, the SSM turns out to be very useful as a benchmark model, since, once the coupling to quarks is fixed, the production cross section can be computed. Extending the SSM to supersymmetry will imply, in the simplest formulation, that the couplings of the Z'_{SSM} to MSSM sfermions and gauginos are the same as the Z . As discussed in Section 2, the Z'_{SSM} coupling to WW pairs must be suppressed, otherwise the WW scattering cross section, mediated by a Z'_{SSM} , would diverge. In the representative point of Ref. [8], the Z'_{SSM} had substantial branching fractions in supersymmetric channels, yielding an overall contribution around 40% to the total decay width.

As in the $U(1)'$ -based analyses, I shall set the Z'_{SSM} mass to the value $m_{Z'} = 2$ TeV and choose a reference point where M_1 , $\tan\beta$ and μ , as well as the trilinear couplings A_q , A_ℓ and A_λ are still the same as in Eqs. (8) and (10). For the sake of obtaining a light Higgs mass of 125 GeV and an interesting phenomenology in supersymmetry, the

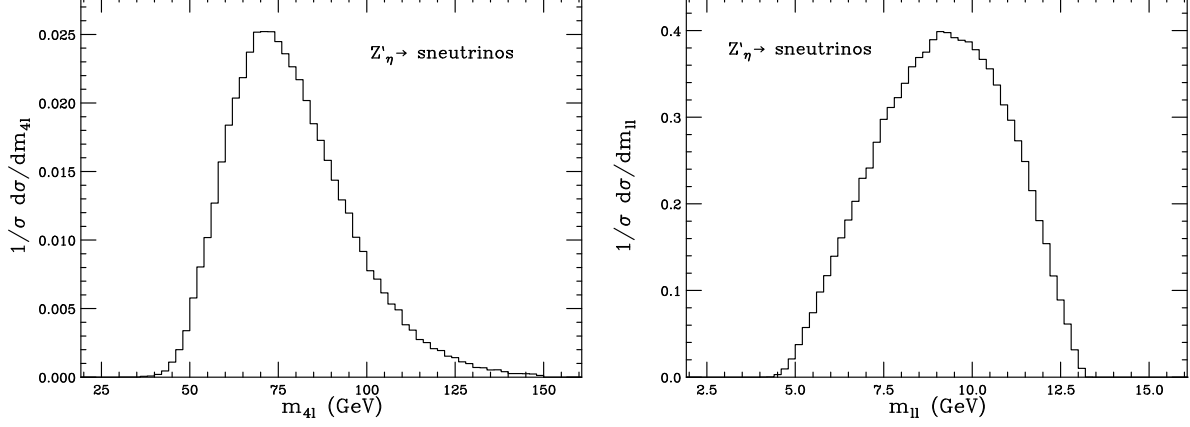


Figure 9: Invariant mass of the four leptons in the process $pp \rightarrow 4\ell + \text{MET}$ (left) and of the $\ell^+\ell^-$ pairs coming from each $\tilde{\chi}_2^0 \rightarrow \tilde{\chi}_1^0 \ell^+ \ell^-$ decay in the cascade (17) (right).

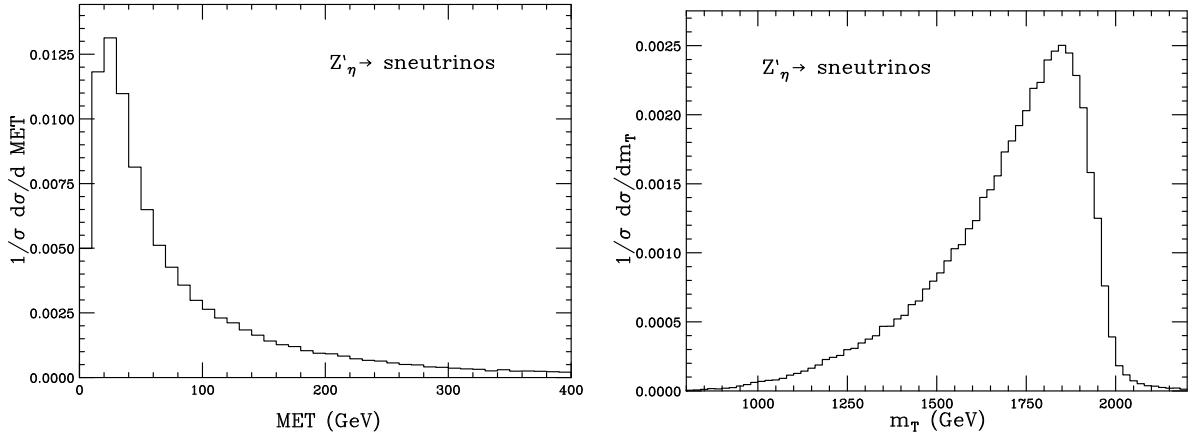


Figure 10: Left: transverse mass for the final state in the process described in Fig. 5). Left: missing transverse energy due to neutrinos and neutralinos

soft sfermion masses at the Z'_{SSM} mass scale will be chosen as:

$$m_{\tilde{\ell}}^0 = m_{\tilde{\nu}_{\ell}}^0 = 500 \text{ GeV} , \quad m_{\tilde{q}}^0 = 5 \text{ TeV} , \quad m_{\tilde{t}}^0 = m_{\tilde{b}}^0 = 1.47 \text{ TeV}, \quad (18)$$

where $m_{\tilde{q}}^0$ is the soft mass of the first two squark generations, i.e. $q = u, d, c, s$, while sbottoms and stops are lighter, as was done in the $U(1)'_{\psi}$ model.

After adding to the quantities in Eq. (18) the D-term correction, one will get the squark and slepton masses quoted in Tables 14 and 15: unlike the cases analyzed before, the impact of the D-term for the chosen SSM point is small and not larger than 5%. In fact, in the SSM the D-term only contains the contribution due to electroweak symmetry breaking, whereas the additional $U(1)'$ term is clearly absent. In the Higgs sector, there is no extra H' , which was instead necessary in the breaking of the $U(1)'$ symmetry, but the particle content is the same as in the MSSM. Their masses are quoted in Table 16: the light h has always mass around 125 GeV and the other three bosons between 630 and 640 GeV.

Table 14: Squark masses in the Sequential Standard Model, in GeV, for the parameters in Eqs. (8), (10) and (18).

$m_{\tilde{d}_1}$	$m_{\tilde{u}_1}$	$m_{\tilde{s}_1}$	$m_{\tilde{c}_1}$	$m_{\tilde{b}_1}$	$m_{\tilde{t}_1}$
5000.3	4999.7	5000.3	4999.7	1480.6	1486.8
$m_{\tilde{d}_2}$	$m_{\tilde{u}_2}$	$m_{\tilde{s}_2}$	$m_{\tilde{c}_2}$	$m_{\tilde{b}_2}$	$m_{\tilde{t}_2}$
5000.0	4999.8	5000.0	4999.8	1460.7	1390.2

Table 15: Slepton masses in the SSM reference point. Numbers are in GeV; all three generations are slightly degenerate.

$m_{\tilde{\ell}_1}$	$m_{\tilde{\ell}_2}$	$m_{\tilde{\nu}_{1,\ell}}$	$m_{\tilde{\nu}_{2,\ell}}$
502.0	502.0	495.0	495.0

The masses of charginos and neutralinos are given in Table 17: unlike the $U(1)'$ models, in the SSM the neutralino sector is the same as in the MSSM, i.e. four $\tilde{\chi}_1^0 \dots \tilde{\chi}_4^0$. With the exception of $\tilde{\chi}_2^{\pm}$ and $\tilde{\chi}_4^0$, the gaugino masses are of the order of a few hundreds GeV and therefore they are light enough to be capable of contributing to the width of a 2 TeV Z'_{SSM} .

Table 16: Masses of the Higgs bosons in the Z'_{SSM} model, for a Z' mass equal to 2 TeV.

m_h	m_H	m_A	m_{H^\pm}
125.8	638.7	632.8	637.8

The branching ratios of the Z'_{SSM} into Standard Model and supersymmetric channels are given in Table 18. The total rate into BSM final states is 27%, with the highest fraction being the one into charginos $\tilde{\chi}_1^+ \tilde{\chi}_1^-$, about 17%; decays into neutralinos and sneutrinos account for about 10%, whereas SM modes are the remaining 73%.

As done for the $U(1)'$ models, the analysis will be carried out for the supersymmetric channel with the highest rate, i.e. the one into chargino pairs, possibly leading to final states with leptons and missing energy, like in Fig. 1. The main chargino branching ratios are quoted in Table 19: the Cabibbo-favoured decays into $\tilde{\chi}_1^0 u \bar{d}$ and $\tilde{\chi}_1^0 c \bar{s}$ are largely dominant, but even those into electrons and muons, i.e. $e^+ \nu_e$ and $\mu^+ \nu_\mu$ pairs, are quite relevant, accounting for about 1/4 of the total Z'_{SSM} rate.

As done previously, the analysis will be undertaken for chargino decays into leptons and light neutralinos, then leading to final states with two charged leptons and missing energy:

$$pp \rightarrow Z'_{\text{SSM}} \rightarrow \tilde{\chi}_1^+ \tilde{\chi}_1^- \rightarrow (\tilde{\chi}_1^0 \ell^+ \nu_\ell) (\tilde{\chi}_1^0 \ell^- \bar{\nu}_\ell), \quad (19)$$

with $\ell = e, \mu$. At $\sqrt{s} = 14$ TeV, the inclusive cross section reads $\sigma(pp \rightarrow Z'_{\text{SSM}}) \simeq 0.63$ pb and the one of the chain (19) is $\sigma(pp \rightarrow Z'_{\text{SSM}} \rightarrow \ell^+ \ell^- + \text{MET}) \simeq 6.18 \times 10^{-3}$ pb, implying about 600 final states with $e^+ e^-$ or $\mu^+ \mu^-$ and missing energy in the phase $\mathcal{L} = 100 \text{ fb}^{-1}$ and even few thousands at 300 fb^{-1} . It is thus confirmed the finding of Ref. [8], where it was observed that the SSM is the scenario which enhances both production cross section and rates into supersymmetric final states.

In Fig. 11 the lepton transverse momentum is presented for primary and secondary lepton production in Z'_{SSM} decays, exhibiting features rather similar to the Z'_ψ case. In $Z'_{\text{SSM}} \rightarrow \ell^+ \ell^-$ events, the normalized differential cross section $1/\sigma(d\sigma/dp_T)$ increases with p_T , is sharply peaked around $p_T \simeq m_{Z'}/2$ and rapidly decreases, so that there are nearly no events for $p_T > 1.3$ TeV. On the contrary, when the leptons are produced through a primary $Z'_{\text{SSM}} \rightarrow \tilde{\chi}_1^+ \tilde{\chi}_1^-$ process, the distribution is sharply peaked in the low p_T range, about $p_T \simeq 11$ GeV, rapidly goes down, being completely negligible for $p_T > 40$ GeV.

The rapidity distribution, presented in Fig. 12 (left) is comparable with Z'_ψ decays, with a higher fraction of events around $\eta = 0$ when the lepton comes from the cascade and at large $|\eta|$ for ℓ^\pm yielded by a direct $Z'_{\text{SSM}} \rightarrow \ell^+ \ell^-$. Even the spectrum of θ (right-

Table 17: Masses of charginos and neutralinos

$m_{\tilde{\chi}_1^+}$	$m_{\tilde{\chi}_2^+}$	$m_{\tilde{\chi}_1^0}$	$m_{\tilde{\chi}_2^0}$	$m_{\tilde{\chi}_3^0}$	$m_{\tilde{\chi}_4^0}$
198.6	835.8	193.5	197.7	413.6	836.0

Table 18: Z'_{SSM} decay rates for $m'_Z = 2$ TeV

Final State	Z' Branching ratio (%)
$\tilde{\chi}_1^+ \chi_1^-$	16.6
$\tilde{\chi}_3^0 \tilde{\chi}_4^0$	3.4
$\sum_i \tilde{\nu}_i \tilde{\nu}_i^*$	4.0
$\tilde{\chi}_2^+ \tilde{\chi}_2^-$	2.5
hZ	2.0
$\sum_i d_i \bar{d}_i$	27.1
$\sum_i u_i \bar{u}_i$	20.7
$\sum_i \nu_i \bar{\nu}_i$	12.2
$\sum_i \ell_i^+ \ell_i^-$	6.1

Table 19: Chargino $\tilde{\chi}_1^+$ decay rates in the reference point for the Z'_{SSM} model.

Final State	$\tilde{\chi}_1^+$ branching ratio (%)
$\tilde{\chi}_1^0 u \bar{d}$	38.9
$\tilde{\chi}_1^0 c \bar{s}$	28.9
$\tilde{\chi}_1^0 e^+ \nu_e$	12.3
$\tilde{\chi}_1^0 \mu^+ \nu_\mu$	12.1
$\tilde{\chi}_1^0 \tau^+ \nu_\tau$	6.5

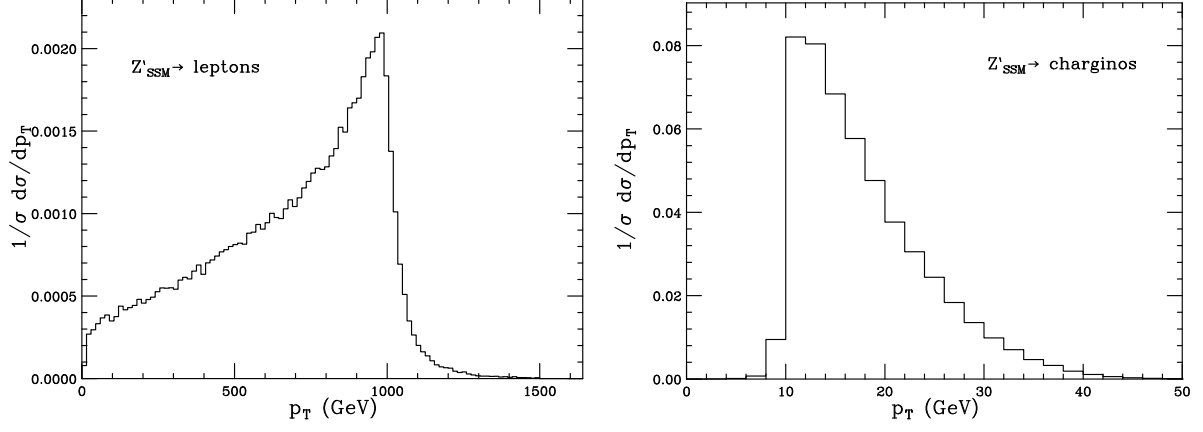


Figure 11: Lepton transverse momentum for the Z'_{SSM} model at $\sqrt{s} = 14$ TeV and $m_{Z'} = 2$ TeV, for a direct $Z'_{\text{SSM}} \rightarrow \ell^+ \ell^-$ decay (left) and a chain initiated by a $Z'_{\text{SSM}} \rightarrow \tilde{\chi}_1^+ \chi_1^-$ (right).

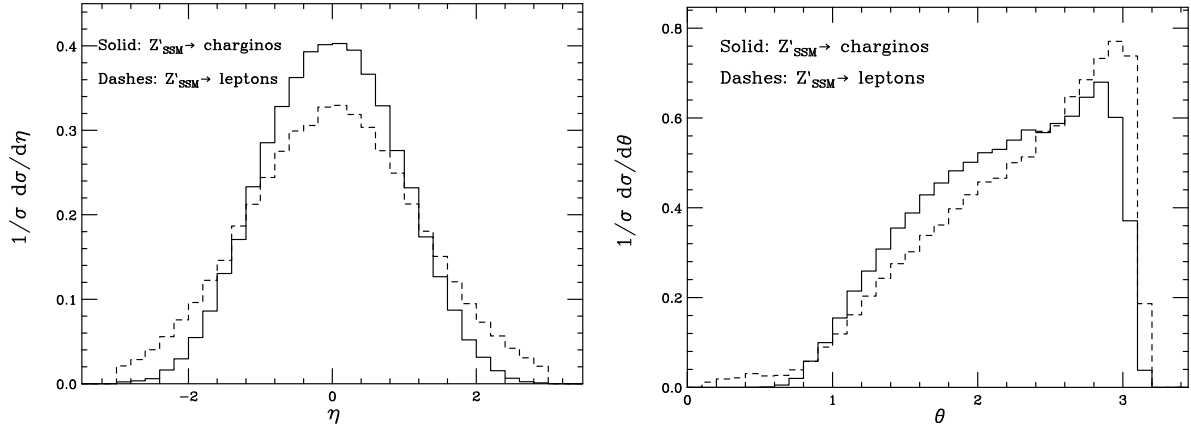


Figure 12: Lepton rapidity (left) and opening angle (right) in Z'_{SSM} decays. The solid histograms refer to the cascade initiated by a decay into chargino pairs, the dashes to direct $Z'_{\text{SSM}} \rightarrow \ell^+ \ell^-$.

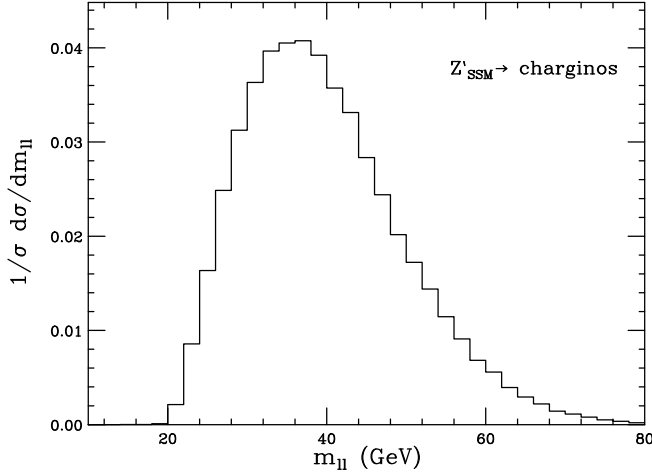


Figure 13: Invariant mass distribution of the two charged leptons in the process (19).

hand side of Fig. 12), the opening angle between ℓ^+ and ℓ^- , qualitatively exhibits the same features as the $U(1)'_\psi$ case: the decay chain (19) yields a broader distribution, with more events for middle θ values and less at small and very high θ . The invariant mass distribution $m_{\ell\ell}$, displayed in Fig. 13, is relevant in the range $20 \text{ GeV} < m_{\ell\ell} < 80 \text{ GeV}$ and reaches its maximum value at $m_{\ell\ell} \simeq 37 \text{ GeV}$. Of course, the $\ell^+\ell^-$ invariant-mass distribution in $Z'_{\text{SSM}} \rightarrow \ell^+\ell^-$ processes is a Breit-Wigner function, peaked at $m_{\ell\ell} \simeq m_{Z'}$, which is instead omitted.

Fig. 14 presents the transverse mass and MET for the leptons and neutralinos in the process initiated by a $Z'_{\text{SSM}} \rightarrow \tilde{\chi}_1^+ \tilde{\chi}_1^-$. The MET spectrum is peaked around 20 GeV and rapidly decreases at larger values, whereas the m_T distribution is broader than in the Z'_ψ scenario, is substantial for $1 \text{ TeV} < m_T < 2.5 \text{ TeV}$ and maximum around the Z'_{SSM} mass, i.e. $m_T \simeq 2 \text{ TeV}$.

7 Conclusions

I presented a phenomenological analysis of supersymmetric Z' decays at the LHC, for $\sqrt{s} = 14 \text{ TeV}$ and a few models, based on GUT-inspired $U(1)'$ symmetries and on the Sequential Standard Model. The MSSM was suitably extended, in order to accommodate the new features due to the $U(1)'$ group and the extra Z' boson, and the reference points in the parameter space were chosen in such a way to recover a light Higgs with mass of 125 GeV and obtain relevant Z' branching ratios in the supersymmetric channels.

Within the GUT-driven models, the analysis was carried out for the so-called $U(1)'_\psi$ and $U(1)'_\eta$ groups, since, even in previous work on supersymmetric Z' decays, they

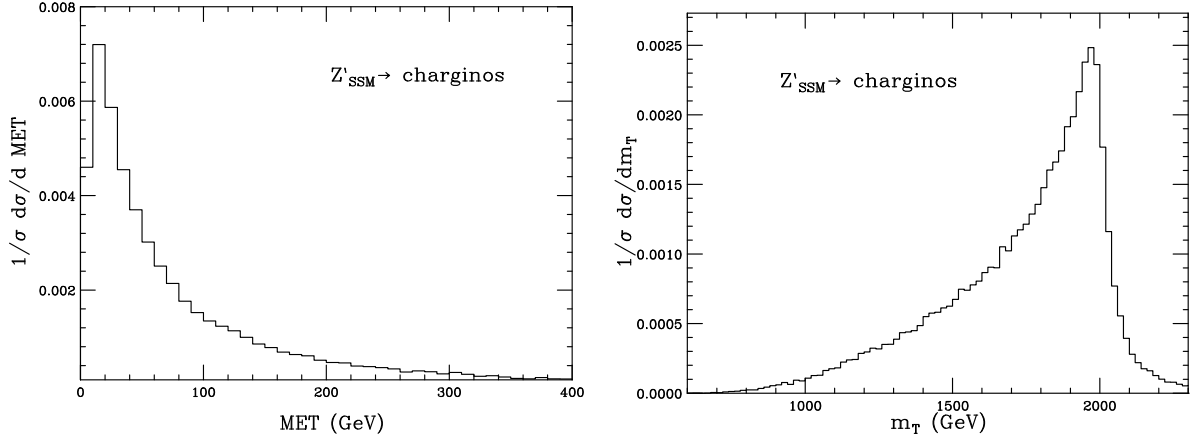


Figure 14: Left: missing transverse energy for the decay chain, initiated by a $Z'_{\text{SSM}} \rightarrow \tilde{\chi}_1^+ \tilde{\chi}_1^-$ primary process, due to the neutralinos $\tilde{\chi}_1^0$ and neutrinos. Right: transverse mass of final states with two charged leptons and missing energy.

were the theoretical scenarios where the supersymmetric signals were enhanced. When fixing the soft squark masses, two options were considered, namely degenerate squarks for all three generations as well as lighter stops and sbottoms with respect to the first two generations. It was found that, in both $U(1)'$ models, for the chosen parameters and $m_{Z'} = 2$ TeV, supersymmetric modes account for about 25-30% of the Z' width, with the decays into chargino and sneutrino pairs yielding the highest supersymmetric branching ratios for the Z'_ψ and Z'_η models, respectively. The Z'_ψ scenario had also a visible rate into the lightest neutralinos $\tilde{\chi}_1^0$, which could be a useful channel to search for Dark Matter candidates.

In the Z'_ψ case, it was then considered a decay chain, initiated by a $Z'_\psi \rightarrow \tilde{\chi}_1^+ \tilde{\chi}_1^-$ process, leading to a final state with two charged leptons and missing transverse energy, due to the production of neutrinos and neutralinos. About $\mathcal{O}(100)$ of such events for luminosities of 100 or 300 fb^{-1} , as expected in the 14 TeV LHC run. The decay into neutralinos ($\tilde{\chi}_1^0 \tilde{\chi}_1^0$) yields an even larger number of events, about $\mathcal{O}(10^3)$ at 14 TeV, and therefore the $U(1)'_\psi$ extension of the MSSM may be worth to be investigated when looking for Dark Matter particles at the LHC. In the Z'_η scenario, the $Z'_\eta \rightarrow \tilde{\nu}_2 \tilde{\nu}_2^*$ process, where $\tilde{\nu}_2$ is mostly a right-handed sneutrino, can give rise to a chain yielding four charged leptons and again missing energy. The expected rate of such events is lower than the Z'_ψ scenario, but still a few dozens of events are expected for pp collisions at 14 TeV. In both $U(1)'$ models, observables like lepton trasverse momentum, rapidity, opening angle and invariant mass, as well as missing transverse energy and transverse mass, are peculiar of supersymmetric decays; the spectra are rather different from those obtained in direct $Z' \rightarrow \ell^+ \ell^-$ processes and, because of the Z' -mass constraint, from other supersymmetry searches.

For the sake of comparison, even the Sequential Standard Model was investigated: in the chosen point of the parameter space, it is still the decay into charginos, leading to final states with two charged leptons and missing transverse energy, the most promising supersymmetric channel. Several hundreds of events are in fact foreseen in the high-energy LHC run, and even $\mathcal{O}(10^3)$ for a luminosity of 300 fb^{-1} . The final-state distributions for the Z'_{SSM} are similar to those obtained for the Z'_ψ , as in both cases one has two charged leptons, neutrinos and neutralinos, but nevertheless some peculiar features, due to the different couplings, are still visible.

In summary, the expected rates and final-state observables would make supersymmetric Z' decays a rather interesting investigation to search for supersymmetry, once the Z' mass were to be known. For the time being, opening the supersymmetric decay channels up will result in lowering the Z' mass exclusion limits, since the expected rates in dilepton pairs decrease. Therefore, although the presented analysis will be useful to search for supersymmetry only after the possible discovery of the Z' , it should be possibly taken into account when determining the Z' mass exclusion limits. Once the data on high-mass leptons are available even at $\sqrt{s} = 14 \text{ TeV}$, it will be very interesting comparing the data with the theory results on the product $\sigma(pp \rightarrow Z') \times \text{BR}(Z' \rightarrow \ell^+ \ell^-)$, as done in [11] for the analysis at 8 TeV, and determine the exclusion limits accounting for supersymmetric decays. However, a complete analysis should necessarily compare possible supersymmetric signals in Z' decays with the backgrounds coming from the Standard Model processes as well as non-supersymmetric Z' decays and include the detector simulation. The computation of the backgrounds and the implementation of detector effects is presently in progress.

Furthermore, beyond the models here investigated, which are among those accounted for in the experimental analyses, it may be worthwhile studying in the near future other scenarios, such as the leptophobic models (see, e.g., the pioneering work in [25] or late studies in [26]), wherein the Z' does couple to quarks, thus allowing production via $q\bar{q} \rightarrow Z'$, but the coupling to leptons is suppressed. Within supersymmetry, the very fact that the Z' is leptophobic necessarily decreases the SM rate and enhances the branching ratios in supersymmetric particles. As Z' decays into charginos and neutralinos played a major role in the analysis here presented, a possible application of this work is in the context of split supersymmetry [27], wherein the scalar particles are much heavier than the gauginos, which are therefore the only supersymmetric particles accessible at colliders. Investigations of leptophobic Z' models as well as of Z' bosons in the framework of split supersymmetry are in progress as well.

Acknowledgements

I am indebted to Simonetta Gentile, coauthor of Ref. [8], who contributed in the early stages of this work. I am especially grateful to Florian Staub and Benjamin Fuks for their unvaluable help in using the SARAH/SPheno and FeynRules/MadGraph codes, respectively, and to Tony Gherghetta for discussions on the results of Ref. [5]. I also acknowledge conversations with Nazila Mahmoudi, Andrea Romanino, Barbara Clerbaux, Hwidong Yoo and Marianna Testa on these and related topics.

References

- [1] P. Langacker, Rev. Mod. Phys. 81 (2009) 1199.
- [2] J.L. Hewett and T.G. Rizzo, Phys. Rep. 183 (1989) 193.
- [3] ATLAS Collaboration, Phys. Rev. D90 (2014) 052005.
- [4] CMS Collaboration, Phys. Lett. B720 (2013) 63.
- [5] T. Gherghetta, T.A. Kaeding, and G.L. Kane, Phys. Rev. D57 (1998) 3178.
- [6] M. Baumgart, T. Hartman, C. Kilic and L.-T. Wang, JHEP 0711 (2007) 084.
- [7] C.-F. Chang, K. Cheung and T.-C. Yuan, JHEP 1109 (2011) 058.
- [8] G. Corcella and S. Gentile, Nucl. Phys. B866 (2013) 293; Erratum-ibid. B868 (2013) 554.
- [9] H.E. Haber and G.L. Kane, Phys. Rep. 117 (1985) 75.
- [10] R. Barbieri, S. Ferrara and C.A. Savoy, Phys. Lett. B119 (1982) 343.
- [11] G. Corcella, EPJ Web of Conf. 60 (2013) 18011.
- [12] K.A. Olive et al. (Particle Data Group), Chin. Phys. C, 38 (2014) 090001.
- [13] ATLAS Collaboration, Phys. Lett. B716 (2012) 547;
CMS Collaboration, Phys. Lett. B710 (2012) 26.
- [14] J. de Blas, J.M. Lizana and M. Perez-Victoria, JHEP 1301 (2013) 166.
- [15] F. Staub, Comput. Phys. Commun. 184 (2013) 1792.
- [16] F. Staub, Comput. Phys. Commun. 185 (2014) 1773.

- [17] W. Porod and F. Staub, *Comput. Phys. Commun.* 183 (2012) 2458.
- [18] A. Alloul, N.D. Christensen, C. Degrande, C. Duhr d, B. Fuks, *Comput. Phys. Commun.* 185 (2014) 2250.
- [19] J. Alwall, M. Herquet, F. Maltoni, O. Mattelaer, T. Stelzer, *JHEP* 1106 (2011) 128.
- [20] G. Corcella et al, *JHEP* 0101 (2001) 010.
- [21] A. Arbey, M. Battaglia, A. Djouadi and F. Mahmoudi, *JHEP* 1209 (2012) 107.
- [22] A. Arbey, M. Battaglia, A. Djouadi and F. Mahmoudi, *Phys. Lett. B* 720 (2013) 153.
- [23] M. Carena, S. Gori, N.R. Shah, C.E.M. Wagner, L.-T. Wang, *JHEP* 1308 (2013) 087.
- [24] J. Pumplin, D.R. Stump, J. Huston, H.L. Lai, Pavel M. Nadolsky, W.K. Tung, *JHEP* 0207 (2002) 012.
- [25] F. del Aguila, M. Quiros and F. Zwirner, *Nucl. Phys. B* 284 (1987) 530.
- [26] C.-W. Chiang, T. Nomura and K. Yagyu, *JHEP* 1405 (2014) 106
- [27] N. Arkani-Hamed and S.Dimopoulos, *JHEP* 0506 (2005) 073. G.F. Giudice and A. Romanino, *Nucl. Phys. B* 699 (2004) 65, Erratum-ibid. B706 (2005) 65.